

REVIEW: THE USE OF NEGATIVE STAINING AND CRYO-ELECTRON MICROSCOPY TO UNDERSTAND THE MOLECULAR MECHANISM OF MYOSIN-LINKED REGULATION OF STRIATED MUSCLE CONTRACTION

Raúl Padrón¹⁺ and Lorenzo Alamo

¹Departamento de Biología Estructural, Instituto Venezolano de Investigaciones Científicas (IVIC), Apdo. 21827, Caracas 1020A, VENEZUELA.

⁺Corresponding author: padron@ivic.ve, tel. +58 212 504-1098, fax +58 212 504-1444

ABSTRACT

The sliding of thick filaments along thin filaments is produced by the active shortening of the striated muscle during contraction, and is controlled by molecular switches in the thin and/or thick filaments. In spite of advances on the elucidation of the molecular mechanism of actin-linked regulation, the myosin-linked regulation mechanism has been less amenable to structural studies, due to the low resolution of the three-dimensional (3D) reconstruction maps. A combination of adequate specimens, an improved negative staining method that preserve myosin heads helices and the use of improved reconstruction techniques, allowed the calculation of a 5 nm resolution 3D-map. This 3D-map was interpreted with the available myosin head structural information, but the fitting of atomic structures remained ambiguous due to the limited resolution. Cryo-electron microscopy (EM) of frozen-hydrated tarantula thick filaments extended resolution to 2.5 nm, and the use of single particle averaging techniques enabled the calculation of a 2.5 nm 3D-map. This 3D-map was interpreted unambiguously by fitting the heavy meromyosin atomic structure to it, leading to the atomic model of the relaxed thick filament, which revealed intra- and intermolecular interactions that keep myosin heads forming helices closer to the backbone surface. EM and X-ray evidences suggested that phosphorylation of myosin regulatory light chains is involved in breaking these interactions, activating the thick filaments by

disordering and releasing the myosin heads, enabling their interaction with thin filaments. This atomic model has opened the way to the understanding of the molecular mechanism of the myosin-linked regulation of striated muscle contraction.

Keywords: Negative_stain, cryo-electron_microscopy, myosin_regulation, thick_filaments, 3D_reconstruction

RESUMEN

El deslizamiento de los filamentos gruesos a lo largo de los filamentos delgados es producido por el acortamiento activo del músculo estriado durante la contracción, la cual es controlada por interruptores moleculares en los filamentos delgados y/o gruesos. A pesar de los avances en la dilucidación del mecanismo molecular de la regulación ligada a actina, el mecanismo de regulación ligado a la miosina ha sido menos accesible a los estudios estructurales, dada la baja resolución de los mapas de reconstrucciones tridimensionales (3D). Una combinación de especímenes adecuados, un método de tensión negativa mejorado que preserva las hélices de cabezas de miosina y el uso de técnicas mejoradas de reconstrucción, permitió el cálculo de un mapa 3D a 5 nm de resolución. Este mapa 3D fue interpretado con la información disponible de la estructura de la cabeza de miosina, pero por la resolución limitada el ajuste de las estructuras atómicas era ambiguo. La crio-microscopía electrónica (ME) de filamentos gruesos de tarántula congelado-hidratados extendió la resolución a 2.5 nm, y el uso de técnicas de promediación de partículas aisladas

permitió el cálculo de un mapa 3D a 2.5 nm. Este mapa 3D fue interpretado de manera no ambigua al ajustar a él la estructura atómica de la meromiosina pesada, obteniéndose el modelo atómico del filamento grueso relajado, el cual reveló interacciones intra- e intermoleculares que mantienen a las cabezas de miosina formando hélices cercanas a la superficie del esqueleto. Evidencias de ME y difracción de rayos-X sugieren que la fosforilación de las cadenas ligeras reguladoras de la miosina esta envuelta en el rompimiento de estas interacciones, activando los filamentos gruesos por el desordenamiento y liberación de las cabezas de miosina, permitiendo su interacción con los filamentos delgados. Este modelo atómico ha abierto el camino para la dilucidación del mecanismo molecular de la regulación ligada a miosina de la contracción de músculo estriado.

INTRODUCTION

Muscle is formed by the overlapping of two different sets of filaments, the thin and the thick filaments. The contraction of muscle occurs when these two sets of filaments slide actively one against the other, shortening the sarcomere¹⁻³. Muscle contraction needs to be controlled or regulated in an effective way such that this force production could be useful for programmed movement. Nervous stimulation causes the release of Ca^{2+} ions from the sarcoplasmic reticulum. The Ca^{2+} ions can control the initiation of muscular contraction through two ways: either by acting on the actin filaments, so-called *thin filament regulation* and/or by acting on the myosin filaments, so-called *thick filament regulation*⁴.

The molecular basis of the actin-linked regulation is well understood, following the advances on the molecular structure of the thin filaments, owed to X-ray diffraction and electron microscopic (EM) studies⁵. Thin filament regulation is mediated by the binding of Ca^{2+} ions to troponin C, and involves -via the action of the troponin complex- the movement of tropomyosin

towards the thin filament groove removing the steric block that hinder the attachment of the myosin heads to the actin molecules. There are two structural states for the thin filaments: the switched OFF state, in which tropomyosin blocks the myosin binding site of the actin molecules; and the switched ON state in which the tropomyosin move away into the groove releasing the myosin binding site. On the other hand, the molecular basis of the myosin-linked regulation is not well understood⁶. Myosin-linked regulation occurs either by the direct binding of Ca^{2+} ions to the myosin light chains, as in scallops⁷; or by the phosphorylation of the myosin regulatory light chains (RLC), which takes place in some invertebrate striated muscles, for instance, in the arthropod chelicerates⁸, as well as in vertebrate striated muscle⁹ and smooth muscle¹⁰. The limiting step to advance towards the understanding of the molecular mechanism of the myosin-linked regulation is the determination of the molecular structure of myosin thick filaments. In this review we summarize how the negative stain technique and the cryo-electron microscopy have contributed to the understanding of the molecular structure of thick filaments from striated muscle, and, how the achieved new structure can help on understanding more about the molecular mechanism of the myosin-linked type of muscle contraction regulation.

The thick filaments of striated muscle are polymers of myosin II. The tails of the myosin molecules are packed together forming a central backbone, whereas the two heads from each myosin molecule are arranged on the surface of the backbone (see reviews in ref. 11 and 12), forming helices in the relaxed state^{13,14,15}. Several reasons have slowed down obtaining high resolution structures of thick filaments: on one hand, technical difficulties on obtaining good native-like preservation of thick filaments by the standard negative stain electron microscopic technique; and on the other, mathematical difficulties on calculating the three-dimensional (3D) helical reconstruction from these images. The species

used has also been a very important factor: the thick filaments from the arthropod chelicerates, especially from the spider (tarantula) leg muscles, are the specimens that have proved to be the most easily preserved specimens for structural studies¹⁶.

During the past 43 years these difficulties have been overcome, and it was in 2005 when the structure of thick filaments at a quasi-atomic molecular resolution was finally achieved¹⁷. To accomplish this final result a method has been developed that allows the rapid freezing of thick filaments preserving the arrangement of myosin heads in helices, as visualized by low electron dose EM¹⁸. However, the attempts to calculate a 3D reconstruction of these frozen-hydrated filaments failed: first, due to the impossibility of separating the overlapped Bessel functions from these low-dose images¹⁹, and secondly, as the preparation of thick filaments contained a large quantity of thin filaments, making the sampling of good areas in the electron micrographs -free of thin filaments- an almost impossible task¹⁹. To overcome this problem a method was developed that permits the isolation of purified thick filaments²⁰. The calculation of the 3D reconstruction of these frozen-hydrated relaxed purified thick filaments¹⁷ was achieved last year by using a new method based on single particle averaging²¹. This technique, named IHRSR, when applied to the chelicerate cryo-EM data reveals a very detailed structure of the thick filament¹⁷ and has provided important structural clues that have opened the way to the understanding of the molecular basis of one type of myosin linked regulation - the one that occurs via the myosin RLC phosphorylation.

THE STRUCTURE OF THICK FILAMENTS FROM STRIATED MUSCLE

The initial insight on the structure of thick filaments from striated muscle was the visualization of vertebrate thick filaments on the electron microscope, the

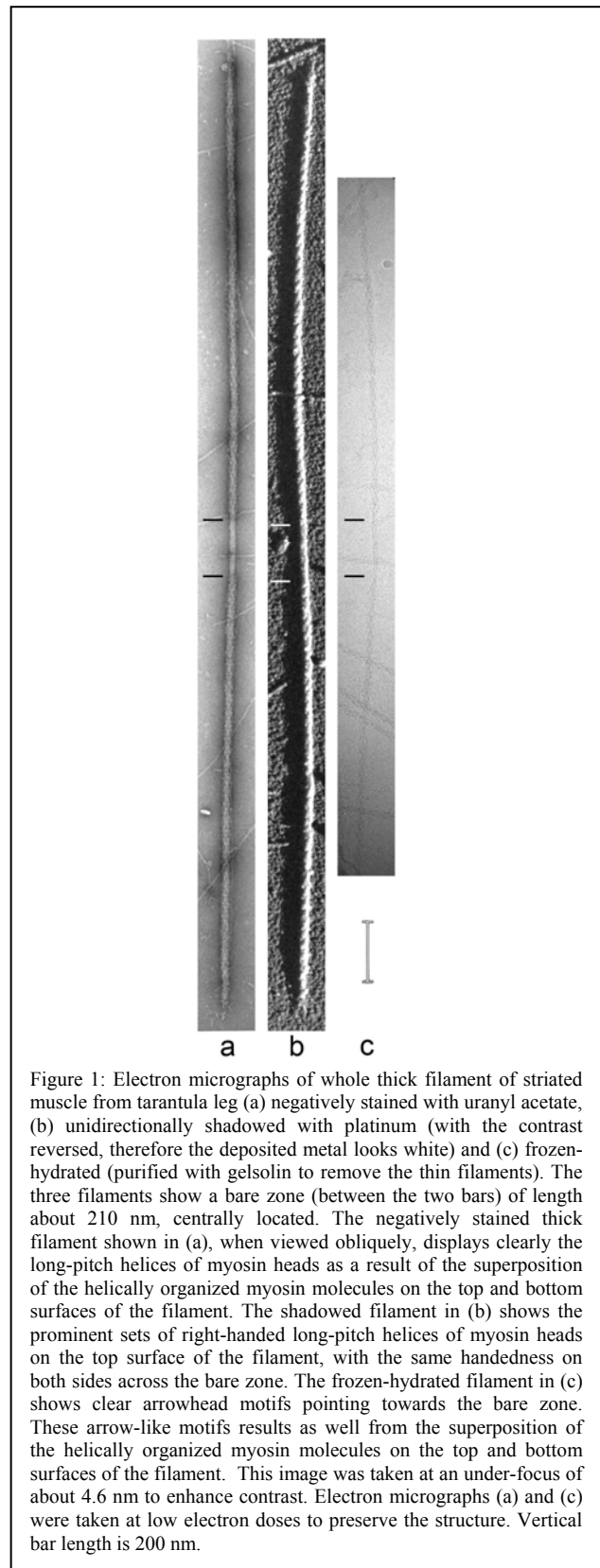


Figure 1: Electron micrographs of whole thick filament of striated muscle from tarantula leg (a) negatively stained with uranyl acetate, (b) unidirectionally shadowed with platinum (with the contrast reversed, therefore the deposited metal looks white) and (c) frozen-hydrated (purified with gelsolin to remove the thin filaments). The three filaments show a bare zone (between the two bars) of length about 210 nm, centrally located. The negatively stained thick filament shown in (a), when viewed obliquely, displays clearly the long-pitch helices of myosin heads as a result of the superposition of the helically organized myosin molecules on the top and bottom surfaces of the filament. The shadowed filament in (b) shows the prominent sets of right-handed long-pitch helices of myosin heads on the top surface of the filament, with the same handedness on both sides across the bare zone. The frozen-hydrated filament in (c) shows clear arrowhead motifs pointing towards the bare zone. These arrow-like motifs result as well from the superposition of the helically organized myosin molecules on the top and bottom surfaces of the filament. This image was taken at an under-focus of about 4.6 nm to enhance contrast. Electron micrographs (a) and (c) were taken at low electron doses to preserve the structure. Vertical bar length is 200 nm.

result of the pioneer work of Hugh Huxley in 1963, who observed for the first time isolated thick filaments from vertebrate striated muscle by negatively staining¹³. He

suggested, based on the thick filament EM images, the first model of a thick filament in which the myosin tails pack together forming the *backbone*, in an anti-parallel way, leaving a central zone (called *bare zone*) naked of myosin heads, which were in the surface of the filaments at both sides of the bare zone.

The next pioneer work was achieved also by Hugh Huxley four years later, when in 1967 he was able to record the low-angle X-ray diffraction pattern of thick filaments²². This diffraction pattern showed a series of layer lines spaced $1/14.3 \text{ nm}^{-1}$ with a meridional reflection at $1/14.3 \text{ nm}^{-1}$, indicating that the myosin heads were arranged in helices with a distance between neighboring myosin heads of 14.3 nm and a helical repeat of 42.9 nm. Despite the important advancement achieved observing that the myosin heads were arranged helically on the surface of the thick filaments, the actual number of helices as well as the myosin head disposition remained unknown, as this information could not be obtained unambiguously from the X-ray diffraction patterns.

During the next 14 years, despite the intense work by several groups, no major advancement was achieved obtaining additional structural information on the thick filaments, either by X-ray diffraction or EM. For unknown reasons, the negative staining method was not good enough to preserve the helical order that was seen in the same conditions by low-angle X-ray diffraction. The myosin heads seen in the negatively stained specimen were completely disordered, as opposed to the helical order detected by X-ray in the same conditions. A breakthrough happened in 1981 when Bob Kensler and Rhea Levine observed for the first time helical order in negatively stained specimens of striated muscle from *Limulus*, an arthropod chelicerate²³. The images from negatively stained thick filament from *Limulus* revealed four helical tracks with a repeat of 43.5 nm in agreement with the X-ray diffraction patterns from *Limulus*¹⁵, and a preliminary 3D helical reconstruction with myosin heads spaced 14.5 nm axially was

reported^{24,25}. Soon the helical order in negatively stained thick filaments from the striated muscle another arthropod chelicerate, tarantula²⁷, as well as from scallops²⁶, were also preserved. For the thick filaments of tarantula a 5 nm 3D helical reconstruction²⁷ was calculated, which was possible due to an algorithm²⁷ programmed to separate the Bessel functions which happen to overlap in the layer lines of the Fourier transforms of the images from the chelicerate thick filaments, which was the problem that hampered achieving the full resolution of the 3D maps. In a short time, using this algorithm, the 5 nm resolution 3D helical reconstruction of *Limulus* and scorpion thick filaments was also calculated²⁸. A new advance occurred when the thick filaments from scallop striated muscle were visualized for the first time in the frozen-hydrated state²⁹ opening the way to increase the actual resolution of the 5 nm negative stain 3D maps. However, as mentioned before it has been for the tarantula muscle in which the joining of different approaches has made possible a final solution of the molecular structure of a striated muscle thick filament, which is the reason we will concentrate in the rest of this review on the studies that have been done with this specific arthropod chelicerate thick filament, that have become an exemplar for the thick filament structure.

The structure of thick filaments from tarantula striated muscle

We soon succeeded in observing by negative staining the presence of helices of myosin heads in relaxed isolated thick filament from striated muscle from tarantula legs¹⁶ (fig. 1a). The electron micrographs showed also in some regions where the myosin heads were disordered, weak 4 nm longitudinal features running parallel to the filament axis¹⁶. At the same time Bob Kensler and coworkers succeeded also in preserving the thick filaments from tarantula muscle³² which they found were similar to the

scorpion and *Limulus* thick filaments. Using metal shadowing we established that these helices were right-handed^{33,34} (fig 1b), and using image analysis we demonstrated that there were 4 helices, succeeding on calculating a 3D helical reconstruction by solving the mentioned problem of the overlapping of Bessel functions^{27,33,34}. By the same time, Rhea Levine and coworkers studied the thick filaments from tarantula muscle³⁵ confirming the results concerning the handedness of the myosin helices, the axial spacing and helical repeat period and the number of helices; and, determining the presence of an extra protein component, the paramyosin, accounting to 24% of the molecules in these filaments, with a paramyosin: myosin heavy chain molecular ratio of 0.31. At that time there was no way to

visualize 3D maps, which were actually built in balsa wood or by staking transparencies of the transverse sections. Therefore, a computer program was written to plot in the new available computer graphics raster displays the surface representation of the thick filament reconstruction as a stack of transverse sections²⁷. This 3D map (fig. 2a), was calculated at an average resolution of 5 nm, and shows 4 helical tracks with detailed information. The reconstructed 3D map was interpreted as formed by the two elongated heads of a myosin molecule; one pointing approximately axially towards the bare zone, and the other pointing in the opposite direction, making a slew angle of about 45 degrees with the axis (fig 2a, top). The envelope of the heads (myosin sub-fragment 1 [S1]) on the reconstruction closely resembled the head

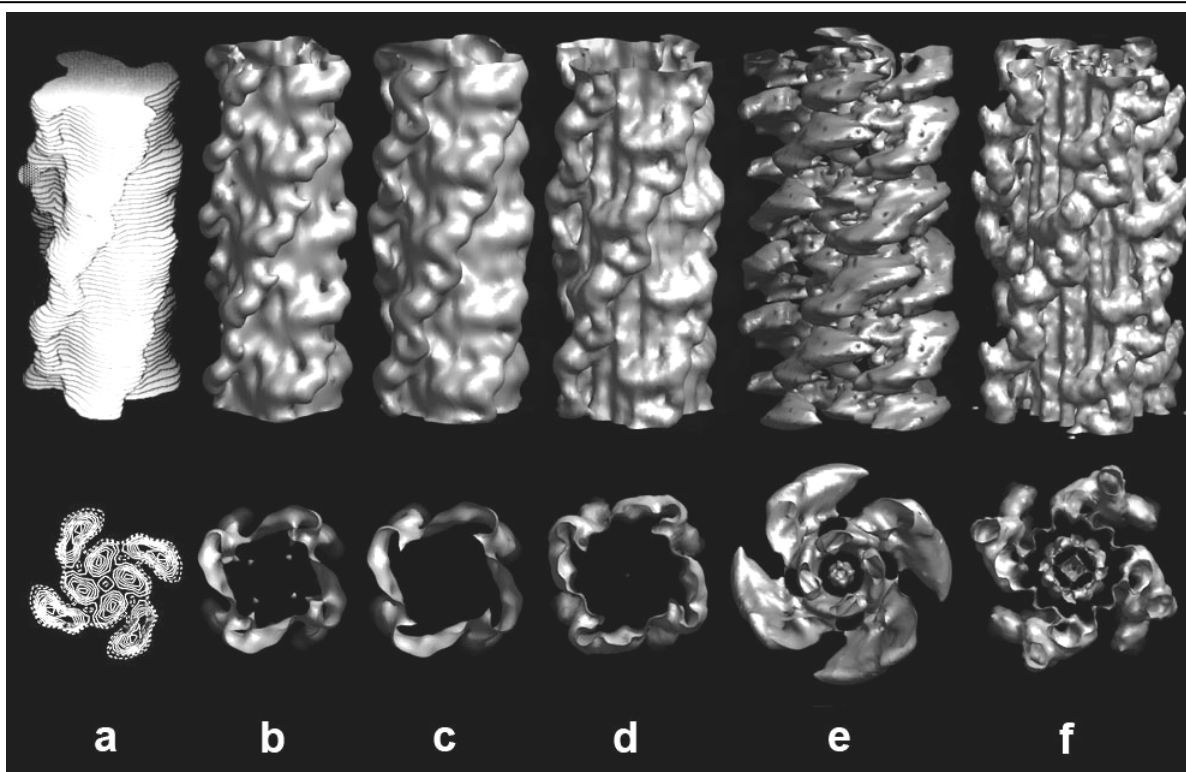


Figure 2: Longitudinal and transverse views of the three-dimensional reconstructions of tarantula thick filaments calculated by different 3D reconstruction techniques (helical reconstruction vs. iterative helical real-space reconstruction²¹ IHRSR) from images visualized with different EM techniques (negative staining vs. frozen hydrated cryo-EM). Negatively stained thick filaments (a-d): the calculated 3D map helical reconstruction (~5 nm resolution), with Bessel function overlapping separation²⁷ as visualized (a) initially with a raster display program²⁷, (b) and (c) are negative staining maps calculated at high and low density contour levels compared with the 3D map (d) calculated with the IHRSR technique²¹ using the same negatively stained data²⁷ (~5 nm resolution at high density contour levels). The maps (b) – (e) were visualized with Chimera⁶⁴ (USCF, University of California). Frozen-hydrated thick filaments (e-f): the calculated averaged (without Bessel function separation) 3D map helical reconstruction (5 nm resolution) (e), and calculated with the IHRSR technique²¹ (2.5 nm resolution) (f). The reconstruction shown in (f) is similar in overall appearance to that determined by helical reconstruction of negatively stained specimens (b,c) and IHRSR (d) but shows dramatic and crucial new details (both in the surface and in the backbone) not previously seen. Transverse sections of each reconstruction (14.5 nm thick) show a 4-fold symmetric arrangement of myosin heads (at high radius); however, only in (f) a ring of twelve 4 nm-diameter subfilaments (arrow) are clearly seen. The J feature is clearly seen in (d) and (f), is apparent in (c), and only the top bar of the “J” is seen on (e). 3D maps are oriented with the bare zone at the bottom. Bar 10 nm.

structure as seen in shadowed pictures of isolated myosin molecules³⁶, the curved shape seen on S1-decorated thin filaments³⁷, and details of the heads seen in isolated thick filaments³⁸ which were the only available structural information on the S1 structure at that time. Our interpretation, therefore, was that the heads were splayed appearing to point in opposite directions along the filament axis and located very close to the filament backbone (fig 2a, bottom). This interpretation of the 3D map densities was not the only one possible, and clearly a higher resolution was indeed needed to interpret unambiguously the thick filament 3D map. Using the same Bessel separation algorithm we reported²⁷, Murray Stewart and coworkers calculated the 3D reconstructions of the related *Limulus* and scorpion³⁹ muscle thick filaments at about the same 5 nm resolution which were interpreted favoring our proposed anti-parallel interpretation²⁷. In subsequent studies we were able to visualize the myosin helices directly *in situ* in sarcomeres of longitudinal sections of whole tarantula muscle⁴⁰, and confirmed with a direct experimental approach that the rotational symmetry was N=4 in transverse sections⁴¹.

The use of improved rendering programs to visualize the tarantula thick filament 3D map (fig 2b) provided a more advanced way to interpret the densities of the map⁴². When Ivan Rayment and coworkers reported in 1993 the atomic structure of S1⁴³ they kindly provided us with images of this atomic structure at approximately similar views as the bilobated features on the 3D map, that we visually 2D fit to it resulting in the first splayed-heads atomic model (fig 5b) of the thick filament⁴². Some time later, Ivan Rayment provided us with the α -carbon atomic coordinates of S1 (fig 3a) which we used to visually fit in 3D (using a stereo viewer) six S1 structures into the 3D envelope of the 3D map (fig 5c) to define more precisely the location of the domains and active sites of the myosin head⁴⁴ as at that time we had no mathematical way to fit it against the 3D map densities. A good fit was only obtained when the

two heads from a myosin molecule ran along the helical tracks anti-parallel to each other with their nucleotide pockets opposed. The arrangement, that was in agreement with bis₂₂ATP cross-linking evidence^{45,46}, suggested a simple mechanism for the stabilization of myosin head helices in relaxed muscle via the formation of intermolecular “dimers” of heads from axially adjacent myosin molecules⁴⁴. One problem of the approach of fitting single S1 structures was that they were not interconnected via the myosin tail coiled-coil α -helices. The other problem was the lack of enough detail in the 3D map surface to identify the region where the myosin sub-fragment 2 (S2) enters into the backbone which was very important to position the myosin heads for the fitting. Therefore, the next step in improving the fitting was to use the new heavy meromyosin (HMM) atomic model⁴⁷ to fit it computationally against the densities (instead of in the envelope as before) of the 3D map (fig 2b). At that time, when exploring the lower density contour levels of the map, the higher radius structural details of the 3D map densities were picked up and described as J-shaped and spur featured⁴⁸ (fig 2c) which we thought had approximately the size and shape of a myosin head⁴⁸. We modeled the surface array of myosin heads on the thick filaments using a model of a two-headed regulated myosin molecule in which the RLCs of the two heads together form a compact head-tail-junction (fig 3b), which was computationally fit against the 3D map densities⁴⁸. In the best model obtained each ridge was formed by the motor domain of a head pointing to the bare zone together with the head-tail junction of a neighboring molecule, with the heads pointing to the Z-disc intermittently occupying the J-position (fig 5d). In this model each motor domain interacted with the myosin essential light chain (ELC) and RLC of the neighboring heads⁴⁸. We claimed that a near-radial spoke in the reconstruction connecting the backbone to one end of the ridge could be identified as the start of the coiled-coil tail⁴⁸.

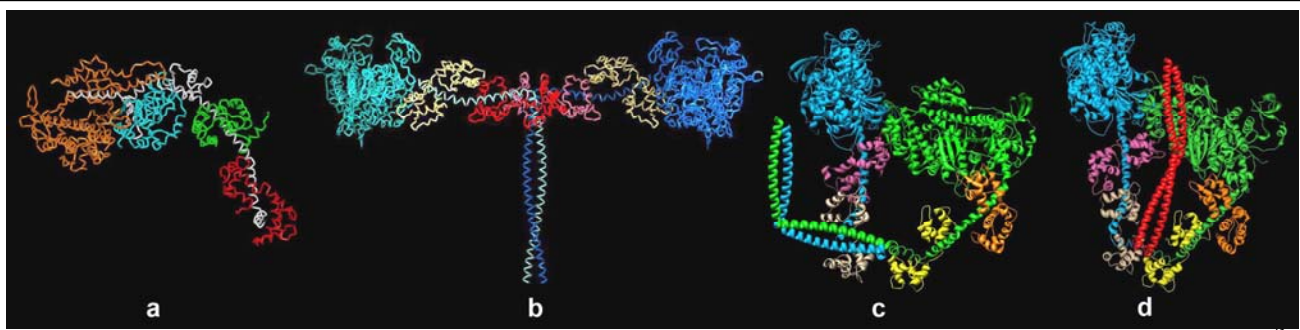


Figure 3: Atomic structure of the myosin molecule used for the fitting to the 3D maps: (a) the myosin sub-fragment 1 (S1) crystallographic structure⁴³ (PDB 1mys) from chicken striated muscle; (b) the symmetric head-tail-junction theoretical model⁴⁸ obtained by adding a head-tail junction model of scallop myosin⁴⁷ by joining the crystal structure of a scallop regulatory domain to a model of the first 102 residues of the scallop coiled coil tail, plus a chicken skeletal motor domain⁴⁵ for each head; (c) the asymmetric “interacting-heads” atomic model^{53,54} (PDB 1i84, left is the “blocked-head”, right is the “free-head”) obtained from EM of 2D-crystals of smooth myosin; and (d) the asymmetric “interacting-heads” atomic model derived for the thick filament of tarantula striated muscle²⁷.

In retrospect, the major problems that hampered the interpretation of the 3D map of the negatively stained thick filament were that the level of structural details has a limited resolution of only 5 nm, and that choosing the cutoff level to be used from the 3D map was not straightforward. The resolution problem is clearly illustrated in figure 4 where it is shown how a hypothetical atomic model for a thick filament (fig 4a, bottom) built from an arbitrary atomic model of a myosin molecule (fig 4a, top) would look in the EM as visualized in the EM by decreasing resolutions (1.2, 5, and 5 nm, fig 4b-d), indicating the unavoidable need to increase the experimental resolution from the 5 nm achievable by negative staining (fig. 4d) to at least up to 2.4 nm (fig 4-c) or better 1.2 nm, fig 4b) to enable an unambiguous interpretation of the 3D map in molecular (or atomic) terms. Therefore our efforts at that time were concentrated in obtaining better preserved specimens imaged at the best possible EM conditions. To preserve the thick filament as well as possible, and to avoid the artifacts that negatively staining produce on them, as for instance the necessary drying, we started to setup a way to rapidly freeze isolated tarantula thick filaments in liquid ethane/propane. Unfortunately the preservation of the helical array, in spite of the important advances achieved in scallop thick filament²⁶, proved not to be an easy task at all; however, we eventually succeeded in obtaining frozen-hydrated thick filaments in the relaxed

state such that the myosin helices were fully preserved, as confirmed by their Fourier transforms¹⁸. The next obstacle we faced after being able to preserve the helical array, which made very difficult to calculate a 3D helical reconstruction¹⁹, was the unexpected increase of the presence of thin filaments in the frozen-hydrated preparations. This problem was solved using the protein gelsolin⁴⁹ to fragment the actin filaments which finally enabled the purification of the thick filaments²⁰. Fig. 1c shows a frozen-hydrated gelsolin-purified tarantula thick filament in the relaxed state, with a 2.4 nm resolution as deduced from the image transforms.

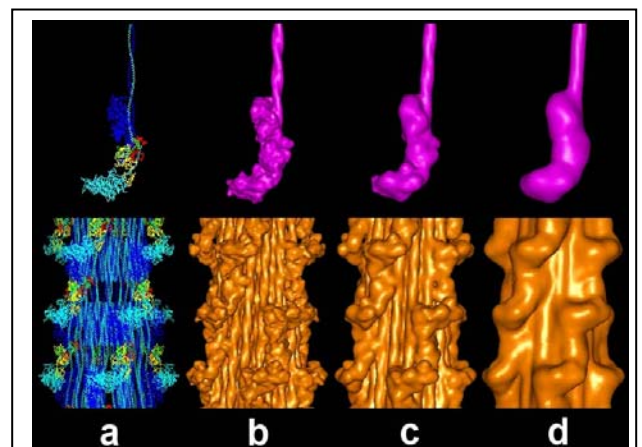


Figure 4: Comparison of how (a) hypothetical atomic models of the myosin molecule (top) and a thick filaments (bottom) should appear when visualized at different spatial resolutions of (b) 1.2 nm, (c) 2.4 nm and (d) 5 nm. In the example of an atomic model of a myosin molecule shown in the top part of (a), one head is arbitrarily pointing up towards the tail and the other pointing down in an opposite way. Only at the resolution of 2.4 nm (c) or higher, 1.2 nm (b) it is possible to unambiguously recognize the details of the single myosin molecule on the 3D map, whereas at the lower resolution of 5 nm (d), that is not possible anymore. It is also clear that the backbone substructure details only begin to be resolved to at least the 2.4 nm (c) resolution.

We worked for a long time on the calculation of the 3D helical reconstruction of the frozen-hydrated thick filament which proved also to be a very difficult task, as separating the overlapping Bessel functions using our original algorithm²⁷ failed due to the weak intensity of the frozen-hydrated images; therefore, unfortunately only an average frozen-hydrated helical reconstruction - without the separation of the overlapped Bessel functions- was possible¹⁹ (fig. 2e) blurring the map details. A very recent and different algorithm⁵⁰ for separating the overlapping of the Bessel functions also failed to work with the tarantula frozen-hydrate EM data. By the year 2000 we decided to try some of the several new algorithms developed to calculate non-helical reconstruction in real space using “single particle” approaches. One of them, developed at Holmes’ lab⁵¹ also failed. The other was the newer approach called “Iterated Helical Real Space Reconstruction” (IHRSR) developed by Ed Egelman²¹ which we could not implement initially after it was published; however, in

2004 we finally succeeded on calculating a preliminary frozen-hydrated 3D map using it. For using this approach, the images from several frozen- hydrated thick filaments were cut in many small image segments (helical particles) and chopped into small fragments containing a bit more than the 43.5 nm repeat distance of the helices. These images are different views of the same “single particle” thick filament. Several thousands of them were classified according to the projections of an initial model (the negative stain 3D map, for instance), averaged, symmetrized and a back-projected using single particle reconstruction algorithms⁵² This first reconstruction was in turn used as a new reference map, and the process was repeated until it converged to a stable 3D map²¹. Three independent 3D maps calculated using the IHRSR technique were indeed very similar. This procedure is a way to avoid the separation of the overlapped Bessel functions as the calculation of the 3D map, as mentioned, is made in real space, without using the Fourier-Bessel helical reconstruction algorithm. The

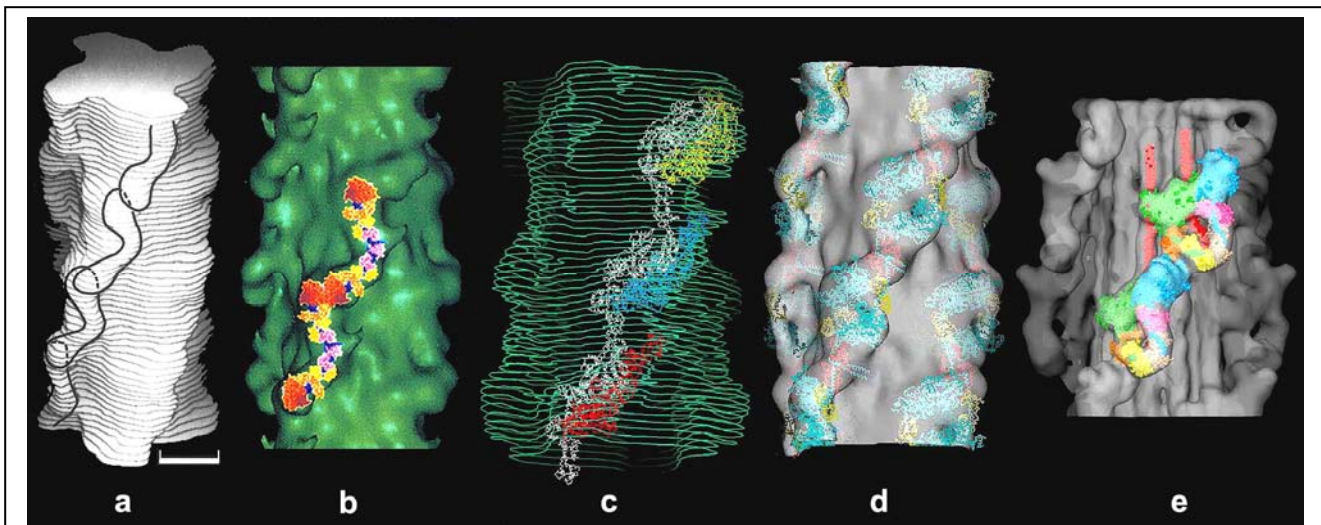


Figure 5: Molecular interpretations of the different calculated 3D maps: Anti-parallel splayed-heads arrangement: (a) first interpretation of the negatively stained (5 nm resolution) 3D map (fig. 2a), based on the visual inspection of how the assumed envelope of the putative heads on the reconstruction resembled the head structure as available in 1984 (shadowed myosin molecules³⁶, head details from isolated thick filaments³⁷ and myosin head curved shaped from S1-decorated thin filaments³⁸), and in which the two elongated heads of a myosin molecule points in opposite directions; (b) similar interpretation by visual 2D fitting of different 2D projections of the S1 structure⁴³ to the better visualized negatively stained 3D map (fig. 2b). Intermolecular dimmers arrangement: (c) single visual stereo 3D-fitting of six α -carbon S1 structures⁴³ to the envelope of the negatively stained 3D map (fig. 2b), also with anti-parallel splayed heads. Intermittently head arrangement: (d) computerized 3D fitting of a symmetric head-tail junction model⁴⁷ to the densities of the negatively stained 3D map⁴⁸ (fig. 2c). Back-paralleled interacting-heads arrangement: visual 3D-fitting of the asymmetric “interacting-heads” atomic model^{53,54} (fig. 3c) to the frozen-hydrated (2.4 nm resolution) 3D map (fig. 2e), in which both heads of a myosin molecule are pointing back to the tail in the direction of the bare zone. This fitting (e) as different to the four (a-d) is unambiguous as -due to the higher resolution achieved- the details on the 3D map can be adjusted precisely with the interacting-heads atomic model (fig. 3c), especially the S2 fragment (arrow), a part of the myosin not seen in the previous 3D maps (fig. 3a-e). Figure (e) was done using Chimera⁶⁴.

new map showed a detailed repeating motif on the surface of the filament (fig. 2f) representing pairs of myosin heads which appears like a “J”. Four of these motifs, equally spaced around the filament circumference, occur at regular axial intervals of 14.5 nm (fig 2f). This 4-fold rotationally symmetric arrangement twists by 30° from one 14.5 nm level to the next, creating four parallel, right-handed, helical tracks, with a helical repeat of 43.5 nm. This new 3D map was interpreted¹⁷ when realizing the close similarity between the shape of this “J” feature with the recently reported “interacting-heads” atomic model of HMM^{53,54} (fig 3c), obtained by EM from 2D crystals of smooth muscle HMM, as shown in fig. 5e. This “interacting-heads” atomic model is in the switched OFF state, with the RLCs dephosphorylated, and the myosin molecule shows an asymmetric interaction between its two heads, with the actin-binding region of one head (the ‘blocked’ head) interacting with the converter and ELC regions of the other (the ‘free’ head)^{53, 54}. This heads-down, pointing to the bare zone interpretation was a completely unexpected surprise, as myosin heads were previously interpreted either as anti-parallel splayed heads²⁷ with one head pointing away from the tail and the other head pointing towards the tail, or parallel heads (see review in ref¹²), both pointing away from the myosin tail; but in no case with both heads pointing in the contrary direction, i.e. towards the tail. This asymmetric interacting-heads atomic structure fits very precisely into the J motif of the reconstruction as confirmed by the 3D fitting of the motor domains and the light chain domains of the two heads (fig 5e), indicating that this structure derived from smooth muscle is also present in the thick filament of striated muscle. This new fitting, as different to the four previous ones shown in figure 5a-d, is unambiguous as –due to the higher resolution achieved– the details on the 3D map can be adjusted precisely with the asymmetric-heads atomic model, and especially the sub-fragment S2, a part of the myosin molecule not seen in the previous 3D maps, and

that we first pointed out clearly¹⁷. The strong similarity between the structures of the myosin molecule isolated from smooth chicken muscle and from tarantula striated muscle suggest that this “interacting-heads” structure may underlie the relaxed state of thick filaments, in both smooth and myosin-regulated striated muscles over a wide range of species¹⁷. On the other hand, the new 3D map¹⁷ revealed (fig. 2f) new details on the backbone of the thick filament not seen before. For the first time it was revealed that the backbone comprise twelve approximately parallel strands, each of ~ 4 nm in diameter (and therefore containing more than one 2 nm diameter myosin tail), centered at a radius of ~8 nm from the filament axis (fig. 2f).

THE MOLECULAR MECHANISM OF MYOSIN-LINKED REGULATION OF MUSCLE CONTRACTION

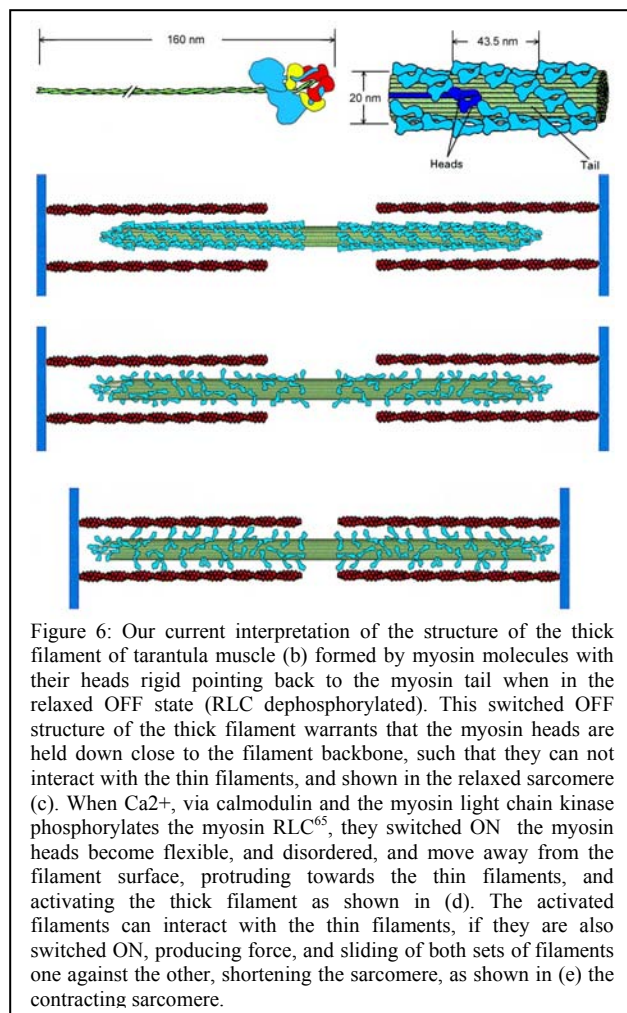
In figure 6 our current thinking is summarized on the structure of the thick filaments of tarantula striated muscle in the relaxed state. Myosin molecules, with their two heads in the asymmetric interacting-heads configuration (fig 6a) are packed together forming the four helices of myosin head pairs (fig 6b) which form the relaxed thick filament (fig 6c). Why do the myosin heads form helices in the relaxed state? The myosin heads form helices because they are in the switched OFF conformation in which both; the blocked head and the free head conformations, are such that specific interacting occurs between them by forming three intramolecular interactions, stabilizing the head pairs; and because the head pairs interact between them by forming two intermolecular interactions, as we have described¹⁷, (shown in detail in figure 7). We have described (fig 7) two intramolecular interactions between the ELC and the converter domain of the free head, the motor domain of the blocked head, and one intramolecular interactions between the S2 and the actin-binding domain of the

blocked head; as well as two intermolecular interactions between the ELC of a blocked head with the actin-binding site of the neighboring head, and between the SH3 domain of the blocked head and the tail of a neighbor molecule¹⁷. Therefore due to these five interactions the thick filament shown in figure 6c which is on the switched OFF state (with the RLCs dephosphorylated) have the myosin heads helically arranged, and packed on top of the backbone surface, away from the thin filaments.

How this increased understanding on the atomic structure of the tarantula thick filaments can help understanding the molecular mechanism of myosin-linked regulation of muscle contraction? As mentioned before the myosin-linked regulation occurs either by the direct binding of Ca^{2+} ions to the myosin light chains, as

in scallops⁷; or by the phosphorylation of the myosin RLCs, as occurs, for instance, in the chelicerates^{8,64}. We think that the determination of the molecular structure of the myosin thick filaments from tarantula muscle can help towards the understanding of the phosphorylation-type of myosin-linked regulation. For the myosin head to interact with the thin filaments, in order to produce the muscle contraction, the thick filaments must first become activated. The activation of the thick filaments is the physiological release of the myosin heads from the thick filament surface just before force development. It is a required intermediate step towards the actual interaction of the myosin heads and the thin filaments.

How are thick filaments activated? When we interpreted the first low resolution tarantula 3D map²⁷ we suggested that the proposed structure (fig 5a) could have implications for contraction mechanisms as indicated by the striking stacking interaction between heads from axially neighboring myosin molecules. We also suggested at that time that in the relaxed state (with dephosphorylated RLCs) the myosin heads were closely associated with the thick filament backbone and with each other, such that this ordered structure was physically locked (such as a “zipper fastener”) through the tips of the heads, helping to maintain the “off” state of the filament, by preventing interaction with actin; and we also speculated that the observed intermolecular interactions could be related to the co-operative switching “on” of filaments that occurs when some muscles are activated⁵⁵ allowing the heads to interact with actin. To test these ideas we explored by negative staining the structural changes associated to the phosphorylation of the myosin RLCs⁵⁶. In these muscles an increase of cytosolic Ca^{2+} led to the RLC phosphorylation via calmodulin and myosin light chain kinase. We found that in the tarantula thick filaments the RLC phosphorylation was accompanied by a loss of order of the helical array of myosin heads characteristic of the relaxed filament, and by a potentiation of the actin



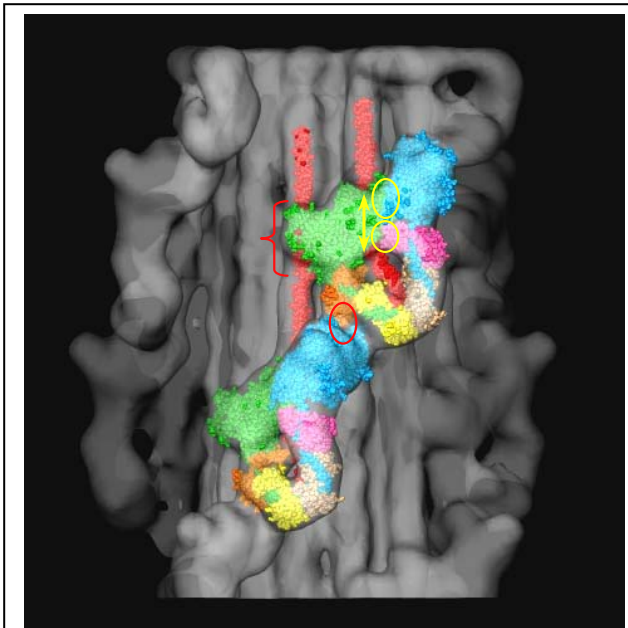


Figure 7: Intra- and intermolecular interactions of myosin heads in the tarantula thick filament¹⁴. The atomic model of the tarantula thick filament reveal¹⁷ three intramolecular interactions, two between the blocked-head actin binding domain and the ELC, and the converter domain of the free-head of the same molecule (yellow ellipsis); and, another between the actin binding domain and the S2 of the same molecule (yellow arrow); and two intermolecular interactions, one interaction between the actin binding domain of the free-head of a myosin head and the ELC of the neighboring blocked-head (red ellipsis), with another interaction between the myosin tail and the SH3 domain of the neighboring blocked-head (red bracket). This figure was done using Chimera⁶⁴.

activation of the myosin Mg-ATPase activity⁵⁶. Therefore, we suggested that in the relaxed state, when the myosin RLC were not phosphorylated, the myosin heads were held down on the filament backbone by head-head interactions, or by interactions of the myosin heads with the filament backbone; whereas the phosphorylation of the myosin RLCs may alter these interactions so that the heads become more loosely associated with the filament backbone giving rise to the observed changes and facilitating the interaction of the heads with the thin filaments. From equatorial X-ray diffraction patterns of tarantula muscles in the phosphorylated state we detected a mass movement in the myosin filaments that supports this finding⁵⁷. Our results were also consistent with a movement of the myosin heads away from the thick filament backbone as modeling suggested that the movement was about 6 nm⁵⁸. Therefore, in tarantula striated muscle, myosin light chain phosphorylation, produces the release and disordering of the myosin heads

and may play a role in facilitation myosin cross bridge interaction with actin. We envisage the activation of the thick filaments as the physiological release of heads from the thick filament surface before force development, as shown in figure 6d; which leads to the actual interaction between the activated myosin heads and the thin filaments, producing contraction and the shortening of the sarcomere (fig 6e). In the case of the tarantula muscle, it is still not clear if the phosphorylation of the RLC directly regulate (as happen in smooth muscle and in *Limulus* for instance) or just modulate the number of myosin heads that become activated: i.e. disordered and closer to interact with the thin filament. This mechanism could be a way to modulate the number of heads involved actively in producing force after a series of twitches in tetanus⁵⁹. In other species that have myosin-linked regulation, like mollusks (scallops), the activation is controlled directly by Ca²⁺ as it has been found that the Ca²⁺ disorders the helical array of myosin heads⁶⁰. This disordering of scallop thick filaments occurs as fast as 30 ms when detected by measurements of the disordering

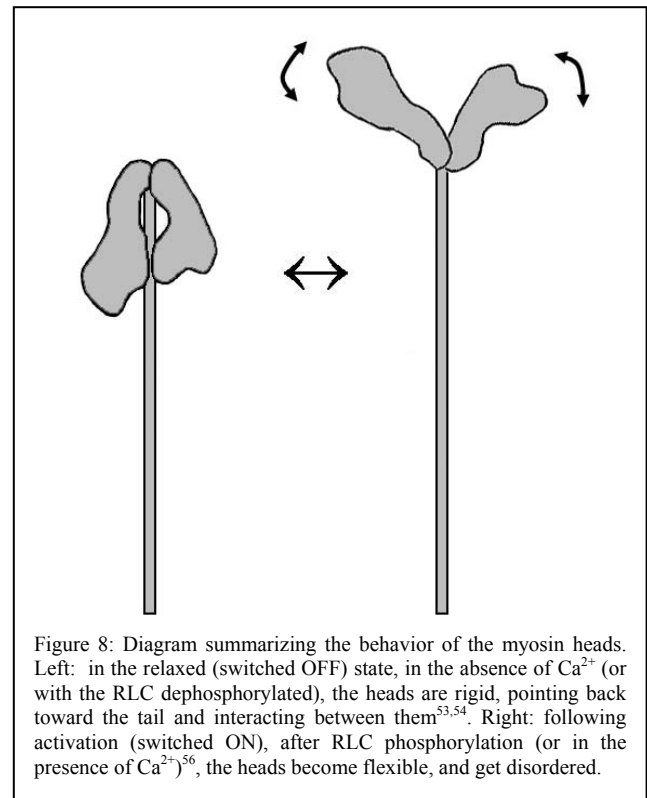


Figure 8: Diagram summarizing the behavior of the myosin heads. Left: in the relaxed (switched OFF) state, in the absence of Ca²⁺ (or with the RLC dephosphorylated), the heads are rigid, pointing back toward the tail and interacting between them^{53,54}. Right: following activation (switched ON), after RLC phosphorylation (or in the presence of Ca²⁺)⁵⁶, the heads become flexible, and get disordered.

time course by rapid negative staining⁶¹, whereas the re-ordering is detected in about 80 ms. For the case of the tarantula thick filaments, our previous results using the standard (static) negative staining technique⁵⁶ indicates that phosphorylation induces disorder in about 5 min., the earliest experimentally detectable time point. So, we can conclude that in the myosin-linked regulated striated muscle, the thick filaments are activated either directly by Ca^{2+} (in mollusks) or by Ca^{2+} via calmodulin and MLCK phosphorylation of the RLCs (in chelicerates).

Why on activation do the myosin heads get disordered and protruded away from the filament backbone following the RLC phosphorylation? Structural evidences on isolated myosin molecules of scallop striated muscle under activation conditions⁶²⁻⁶³ indicates that in the relaxed switched OFF state the two heads of a myosin molecule are held down towards it tails forming a rigid structure with low ATPase activity, and that when they are switched ON by the binding of Ca^{2+} it causes random flexing of the heads around the junction with the tail as summarized in fig 8. In the tarantula thick filament, a similar situation can take place, suggesting that the intra and intermolecular interactions, as well as the intermolecular interaction shown in figure 7 are -in some degree- diminished or broken after the RLCs are phosphorylated. Thus the head-head interactions previously observed in single molecules⁵³⁻⁵⁴, and suggested to be the structural mechanism by which actomyosin ATPase is switched OFF, is also a key feature of the relaxed native filament. Further experiments in which the resolution of the tarantula 3D map is increased enough using field emission gun (FEG) cryo-microscopy or cryo-tomography should help to define more precisely the specific nature of the intra- and intermolecular interactions involved in the activation mechanism.

CONCLUSIONS

The structure of thick filaments of striated muscle in the relaxed state has been finally understood at a quasi-atomic molecular level. The structure reveals intra- and intermolecular interactions that keep heads together forming helices close to the surface of the backbone of the thick filament of striated muscle from tarantula. The similarity between the structure of the myosin molecule in a 2D crystal from a vertebrate smooth muscle and in a thick filament from an invertebrate striated muscle suggest that the intramolecular, interacting head structure may be a general motif for the relaxed state of phosphorylation regulated myosin filaments in smooth and striated muscles of many species. Evidence suggests that the RLC phosphorylation induce the weakening and/or breaking of these interactions allowing the activation of the thick filaments, producing the disordering and releasing out of the myosin heads, and enabling their interaction with the thin filaments. These results have opened the way to understand the molecular mechanism of myosin-linked regulation of muscle contraction.

ACKNOWLEDGEMENTS

We thank Dr. Rodrigo Medina for his help on figure 4. We acknowledge the support of a grant from FONACIT, Venezuela (to R.P.). The research of R. P. was supported in part by an International Research Scholar grant from the Howard Hughes Medical Institute, U. S. A.

PERMISSIONS

Figures 1(a), 2(a) and 5(a) are reprinted from J. Mol. Biol., volume 184, Crowther, R. A., Padrón, R. & Craig, R. Arrangement of the heads of myosin in relaxed thick

Padrón, R. and Álamo, L.

filaments from tarantula muscle, pages 429 – 439, Copyright (1985) with permission from Elsevier. Figure 2(b) and 5(b) reprinted from *J. Struct. Biol.*, volume 115, Padrón, R., Alamo, L., Guerrero, J. R., Granados, M., Uman, P. & Craig, R. Three dimensional reconstruction of thick filaments from rapidly frozen, freeze substituted tarantula muscle, pages 250 – 457, Copyright (1995) with permission from Elsevier. Figures 3(b) and 5(d) reprinted from *J. Mol. Biol.* volume 298, Offer, G.; Knight, P.; Burgess, S. A. Alamo, L. & Padrón, R. A new model for the surface arrangement of myosin molecules in heads in tarantula-thick filaments, pages 239 – 260, Copyright (2000) with permission from Elsevier. Figure 5(c) reprinted from *J. Mol. Biol.* volume 275, Padrón, R.; Alamo, L.; Murgich, J. & Craig, R. Towards an atomic model of the thick filament of muscle, pages 35 – 41, Copyright (1998) with permission from Elsevier. Figure 6 reprinted from *Investigación y Ciencia* (Spanish version of *Scientific American*). Padrón, R. El modelo atómico del filamento de miosina. in press, with permission from *Prensa Científica*, S. A.

REFERENCES

- [1] Huxley H. E., Hanson J. (1954) “Changes in the cross-striations of muscle during contraction and stretch and their structural interpretation” *Nature* 173:973 – 976
- [2] Huxley A. F., Niedergerke R. (1954) “Structural changes in muscle during contraction. Interference microscopy of living muscle fibres” *Nature* 173:971–972
- [3] Geeves M. A., Holmes K. C. (1999) “Structural mechanism of muscle contraction” *Annu Rev Biochem* 68: 687 – 728
- [4] Lehman W., Szent-Gyorgyi A. G. (1975) “Regulation of muscular contraction. Distribution of actin control and myosin control in the animal kingdom” *J Gen Physiol* 66:1-30
- [5] Brown J. H., Cohen C. (2005) “Regulation of muscle contraction by tropomyosin and troponin: how structure illuminates function” *Adv in Protein Chem* 71:121-159
- [6] Kendrick-Jones J., Scholey J. M. (1981) “Myosin-linked regulatory systems” *J Muscle Res Cell Motil* 2:347–372
- [7] Szent-Györgyi A. G., Kalabokis V. N., Perreault-Micale, C. L. (1999) “Regulation by molluscan myosins” *Mol Cell Biochem* 190:55-62
- [8] Sellers J. R. (1981) “Phosphorylation-dependent regulation of *Limulus* myosin. *J. Biol. Chem.* 256:9274-9278
- [9] Szczesna D. (2003) “Regulatory light chains of striated muscle myosin: Structure, function and malfunction” *Current Drug Targets Cardio & Haemat Dis* 3:57-70
- [10] Adelstein R. S., Eisenberg E. (1980) “Regulation and kinetics of the actin-myosin-ATP interaction” *Annu Rev Biochem* 49:921-956
- [11] Craig R., Padrón, R. (2004) “Molecular Structure of the Sarcomere” In *Myology* (eds. Engel, A.G. & Franzini-Armstrong, C.) Chapter 7, New York, McGraw-Hill, pp. 129–166
- [12] Squire J. M., Al-Khayat H. A., Knupp C., Luther P. (2005) “Molecular architecture in muscle contractile assemblies” *Adv in Protein Chem* 71:17-87
- [13] Huxley H. E. (1963) “Electron microscope studies on the structure of natural and synthetic protein filaments from striated muscle” *J Mol Biol* 7:281-308
- [14] Huxley H. E., Brown, W. “The low-angle x-ray diagram of vertebrate striated muscle and its behavior during contraction and rigor” (1967) *J Mol Biol* 30:383-434
- [15] Wray J. S., Vibert P. J., Cohen, C. (1975) “Diversity of cross-bridge configurations in invertebrate muscles” *Nature* 257:561-564

- [16] Craig R., Padrón, R. (1982) "Structure of tarantula muscle thick filaments" *J Muscle Res Cell Motil.* 3(4):487
- [17] Woodhead J. L., Zhao F. Q., Craig R., Egelman E. H., Alamo L., Padrón, R. (2005) "Atomic model of a myosin filament in the relaxed state" *Nature* 436:1195-1199
- [18] Alamo L., Craig R., Horowitz, R., Padrón R. (1999) "Frozen-hydrated thick filaments from tarantula muscle" "25 Years of Cryo-Electron Microscopy of Biological Macromolecules" Florida State University, U.S.A.
- [19] Padrón R., Alamo L., Craig R. (1999) "Three-dimensional reconstruction of frozen-hydrated thick filaments from tarantula muscle" *Biophys J* 76(1):A34
- [20] Hidalgo C., Padrón R., Horowitz R., Zhao F. Q., Craig, R. (2001) "Purification of native myosin filaments from muscle" *Biophys J* 81:2817-2826
- [21] Egelman E. H. (2000) "A robust algorithm for the reconstruction of helical filaments using single-particle methods" *Ultramicroscopy* 85:225-234
- [22] Huxley H. E., Brown, W. (1967) "The low-angle X-ray diagram of vertebrate striated muscle and its behaviour during contraction and rigor" *J Mol Biol* 30:383-434
- [23] Kensler R. W., Levine R. J. C. (1981) *Biophys J* 33:242a
- [24] Stewart M., Kensler R. W., Levine R. J. C. (1981) "Structure of *Limulus* telson muscle thick filaments" *J Mol Biol* 153:781-790
- [25] Kensler R. W., Levine, R. J. (1982) "An electron microscopic and optical diffraction analysis of the structure of *Limulus* telson muscle thick filaments" *J Cell Biol* 92:443-451
- [26] Vibert P., Craig R. (1983) "Electron microscopy and image analysis of myosin filaments from scallop striated muscle" *J Mol Biol* 165:303-320
- [27] Crowther R. A., Padrón R., Craig R. (1985) "Arrangement of the heads of myosin in relaxed thick filaments from tarantula muscle" *J Mol Biol* 184:429-439
- [28] Stewart M., Kensler R. W., Levine R. J. (1985) "Three-dimensional reconstruction of thick filaments from *Limulus* and scorpion muscle" *J Cell Biol* 101:402-411
- [29] Vibert P. (1992) "Helical reconstruction of frozen-hydrated scallop myosin filaments" *J Mol Biol* 223:661-671
- [30] Wray J. S. (1982) "Organization of myosin in invertebrate thick filaments". In *Basic Biology of Muscles: A Comparative Approach.* (Eds. Twarog B. M., Levine R. J. C., Dewey M. M.) New York Raven Press, pp 29-36
- [31] Wray J. S. (1979) "Structure of the backbone in myosin filaments of muscle" *Nature* 277:37-40
- [32] Kensler R. W., Levine R. J. C., Reedy M, Hofmann W. (1982) "Arthropod thick filament structure. *Biophys J* 37: 34a
- [33] Padrón R., Crowther R. A., Craig R. (1983) "Reconstrucción tridimensional de filamentos gruesos de músculo de tarántula" *Acta Cient Venez* 34(1):208
- [34] Padrón R., Crowther R. A., Craig R. (1984) "Three dimensional reconstruction of native tarantula muscle thick filaments" *Biophys J* 45(2):10a
- [35] Levine R. J. C., Kensler R. W., Reedy M. C., Hofmann, W., King, H. A. (1983) "Structure and Paramyosin content of tarantula thick filaments" *J Cell Biol* 97:186-195
- [36] Elliott A., Offer G. (1978) "Shape and flexibility of the myosin molecule" *J Mol Biol* 123:505-519
- [37] Taylor K. A., Amos, L. A. (1981) "A new model for the geometry of the binding of myosin crossbridges to muscle thin filaments" *J Mol Biol* 147:297-324
- [38] Knight P., Trinick J. (1984) "Structure of the myosin projections on native thick filaments from vertebrate skeletal muscle" *J Mol Biol* 177:461-482

Padrón, R. and Álamo, L.

- [39] Stewart M., Kensler R. W., Levine R. J. C. (1985) "Three-dimensional reconstruction of thick filaments from *Limulus* and scorpion muscle" *J Cell Biol* 101:402-411
- [40] Padrón R., Granados M., Alamo L., Guerrero J. R., Craig R. (1992) "Visualization of myosin helices in sections of rapidly frozen relaxed tarantula muscle" *J Struct Biol* 108:269-276
- [41] Padrón R., Guerrero J. R., Alamo L., Granados M., Gherbesi N., Craig R. (1993) "Direct visualization of myosin filament symmetry in tarantula striated muscle by electron microscopy" *J Struct Biol*: 111:17-21
- [42] Padrón R., Alamo L., Guerrero J. R., Granados M., Uman P., Craig R. (1995) "Three dimensional reconstruction of thick filaments from rapidly frozen, freeze substituted tarantula muscle" *J Struct Biol*: 115:250-257
- [43] Rayment I., Rypniewski W. R., Schmidt-Bäse K., Smith R., Tomchick D. R., Benning M. M., Winkelmann D. A., Wesenberg G., Holden H. M. (1993) "Three-Dimensional structure of myosin subfragment-1: a molecular motor" *Science* 261:50-58
- [44] Padrón R., Alamo, L., Murgich, J., Craig, R. (1998) "Towards an atomic model of the thick filament of muscle" *J Mol Biol* 275:35-41
- [45] Levine R. J. C., Chantler P. D., Kensler R. W. (1988) "Arrangement of myosin heads on *Limulus* thick filaments" *J Cell Biol* 107:1739-1748
- [46] Levine R. J. C. (1993) "Evidence for overlapping myosin heads on relaxed thick filaments of fish, frog, and scallop striated muscles" *J Struct Biol* 110:99-110
- [47] Offer G., Knight P. (1996) "The structure of the head-tail junction of the myosin molecule" *J Mol Biol* 256:407-416.
- [48] Offer G., Knight P., Burgess S. A., Alamo L., Padrón R. (2000) "A new model for the surface arrangement of myosin molecules in heads in tarantula thick filaments" *J Mol Biol* 298:239-260
- [49] Yin H. L., Stossel T. P. (1979) "Control of cytoplasmic actin gel-sol transformation by gelsolin, a calcium-dependent regulatory protein" *Nature* 281:583-586
- [50] Wang H. W., Nogales E. (2005) "An iterative Fourier-Bessel algorithm for reconstruction of helical structures with severe Bessel overlap" *J Struct Biol* 149:65-78
- [51] Holmes K. C., Angert I., Kull J. F., Jahn W., Schroder R. (2003) "Electron microscopy shows how strong binding of myosin to actin releases nucleotide" *Nature* 425: 423-427
- [52] Frank J., Radermacher M., Penczek P., Zhu J., Li Y., Ladjadj M., Leith A. (1996) "SPIDER and WEB: processing and visualization of images in 3D electron microscopy and related fields" *J Struct Biol* 116:190-199
- [53] Wendt T., Taylor D., Trybus K. M., Taylor K. (2001) "Three-dimensional image reconstruction of dephosphorylated smooth muscle heavy meromyosin reveals asymmetry in the interaction between myosin heads and placement of subfragment 2" *Proc Natl Acad Sci USA* 98:4361-4366
- [54] Liu J., Wendt T., Taylor D., Taylor, K. (2003) "Refined model of the 10S conformation of smooth muscle myosin by cryo-electron microscopy 3D image reconstruction" *J Mol Biol* 329: 963-972
- [55] Chantler P. D., Sellers J. R., Szent-Gyorgyi A. G. (1981) "Cooperativity in scallop muscle" *Biochemistry* 20:210-216
- [56] Craig R., Padrón R., Kendrick-Jones, J. (1987) "Structural changes accompanying phosphorylation of tarantula muscle thick filaments" *J Cell Biol* 105:1319-1327
- [57] Padrón R., Panté N., Sosa H., Kendrick-Jones, J. (1991) "X ray diffraction study of the structural

- changes accompanying phosphorylation of tarantula muscle” *J Muscle Res Cell Motil* 12:235-241
- [58] Panté N., Sosa H., Padrón R. (1988) “Estudio por difracción de rayos X de los cambios estructurales que acompañan la fosforilación de los filamentos gruesos de músculo de tarántula” *Acta Cient Ven* 39(3):230-236
- [59] Sweeney H. L., Bowman, B. F., Stull, J. T. (1993) “Myosin light chain phosphorylation in vertebrate striated muscle: regulation and function. *Am J Phys Cell Physiol* 264:C1085-C1095
- [60] Vibert P., Craig R. (1985) “Structural changes that occur in scallop myosin filaments upon activation” *J Cell Biol* 101:830-837
- [61] Zhao F., Craig R. (2003) “Ca²⁺ causes release of myosin heads from the thick filament surface on the milliseconds time scale” *J Mol Biol* 327:145-158
- Acta Microscópica*, Vol.13, Nos. 1 y 2, 2004, pp. 14-29
- [62] Stafford W. F., Jacobsen M. P., Woodhead J., Craig R., O’Neill-Hennessey E., Szent-Györgyi A. G. (2001) “Calcium-dependent structural changes in scallop heavy meromyosin” *J Mol Biol* 307:137–147
- [63] Burgess S. A., Yu R., Walker M., Trinick J., Chalovich M., Knight P. (2002) ”Structure of smooth muscle myosin in the switched-off state” *Biophys J* 82:356a
- [64] Pettersen E. F., Goddard T. D, Huang C.C., Couch G.S., Greenblatt D.M., Meng E.C., Ferrin T.E. (2004) “UCSF Chimera - a visualization system for exploratory research and analysis” *J Comput Chem* 25:1605-1612
- [64] Hidalgo C., Craig R., Ikebe M., Padrón R (2001) “Mechanism of phosphorylation of regulatory light chain of myosin from tarantula striated muscle” *J Muscle Res Cell Motil* 22:51-59